ACS OMEGA

Article

Cite This: ACS Omega 2017, 2, 7305-7312

http://pubs.acs.org/journal/acsodf

Enzymatic Catalysis at Nanoscale: Enzyme-Coated Nanoparticles as Colloidal Biocatalysts for Polymerization Reactions

Lucas Philipp Kreuzer,[†] Max Julius Männel,[†,∥] Jonas Schubert,[†,∥,#] Roland P. M. Höller,[†,∥,#] and Munish Chanana*[,†,‡,§]

[†]Physical Chemistry II, University of Bayreuth, Universitätsstr. 30, 95440 Bayreuth, Germany

[‡]Institute of Building Materials, ETH Zürich, Stefano-Franscini-Platz 3, 8093 Zürich, Switzerland

[§]Laboratory for Applied Wood Materials, EMPA Dübendorf, Ueberlandstr. 129, 8600 Dübendorf, Switzerland

[∥]Leibniz Institute for Polymer Research, Hohe Str. 6, 01069 Dresden, Germany

[#]Physical Chemistry of Polymer Materials, Technische Universität Dresden, D-01062 Dresden, Germany

Supporting Information

ABSTRACT: Enzyme-catalyzed controlled radical polymerization represents a powerful approach for the polymerization of a wide variety of water-soluble monomers. However, in such an enzyme-based polymerization system, the macromolecular catalyst (i.e., enzyme) has to be separated from the polymer product. Here, we present a compelling approach for the separation of the two macromolecular species, by taking the catalyst out of the molecular domain and locating it in the colloidal domain, ensuring quasi-homogeneous catalysis as well as easy separation of precious biocatalysts. We report on gold nanoparticles coated with horseradish peroxidase that can catalyze the polymerization of various monomers (e.g., *N*-isopropylacrylamide), yielding thermoresponsive polymers. Strikingly, these biocatalyst-coated nanoparticles can be recovered completely and reused in more than three independent polymerization cycles, without significant loss of their catalytic activity.

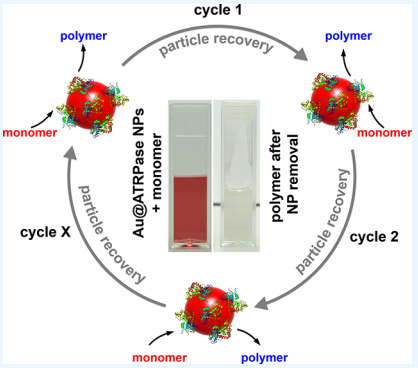

INTRODUCTION

Enzymes represent a family of nontoxic, environmentally friendly catalysts, which have proven to be a powerful tool in the polymerization of a wide variety of monomers and macromonomers.[1−3] Recent publications even demonstrate the use of peroxidases such as horseradish peroxidase (HRP), catalase from bovine liver, and laccase from trametes versicolor as biocatalysts in controlled radical polymerizations.[4−8] For the separation of the two macromolecular species, centrifugal filters with different molecular weight cutoffs can be employed, given that the molecular weight of the catalytic enzyme is different from that of the polymer product.[6,7]

One alternative and highly compelling approach for the separation of the two macromolecular species is to take one of the protagonists, preferentially the catalyst, out of the molecular domain and locate it in the colloidal domain, ensuring quasi-homogeneous catalysis as well as easy separation. This can be achieved by immobilizing the enzymes onto nanoparticles (NPs). In particular, metal and metal oxide NPs in the size range of 5−200 nm fulfill most of the desired requirements: (1) quasi-homogeneous catalysis as their dimension is on the nanoscale and their physical properties, such as diffusion constants, lie between molecular and colloidal domains,[9−12] thus ensuring higher reaction rates than heterogeneous catalysis; (2) high surface/volume ratio, ensuring relatively high catalyst concentration in the immobilized state;[13,14] and the last but not least (3) a simple and straightforward separation from the product by various techniques like centrifugation,[15−17] or in the case of magnetic NPs by magnetic separation.[18]

In general, proteins and enzymes can be immobilized onto solid supports using various techniques,[13,19,20] such as (a) "multipoint" covalent bonding via click chemistry[20−22] or coupling reactions, yielding amide[23−25] or imine bonds,[26−28] (b) cross-linking,[29] (c) affinity immobilization,[30,31] (d) entrapment,[32,33] and (e) adsorption.[15,16,34,35] Depending on the immobilization technique, the immobilization can enhance the properties of enzymes in terms of thermal stability, tolerance to extreme pH, and organic solvents.[36] Therefore, immobilized enzymes can appear to have higher activities than native enzymes under drastic conditions due to the enhanced stability.[34,36−42] On the other hand, the apparent activity of conventional immobilized enzymes can also be lower than that of their native counterparts, mainly because of the hindered substrate accessing or unfavorable conformational transition of the enzyme on the support.[13,43−46] Particularly in the case of colloidal supports, the catalytic performance of the immobilized enzymes also strongly depends on the colloidal stability of the

Received: May 29, 2017
Accepted: September 27, 2017
Published: October 27, 2017

DOI: 10.1021/acsomega.7b00700
ACS Omega 2017, 2, 7305−7312

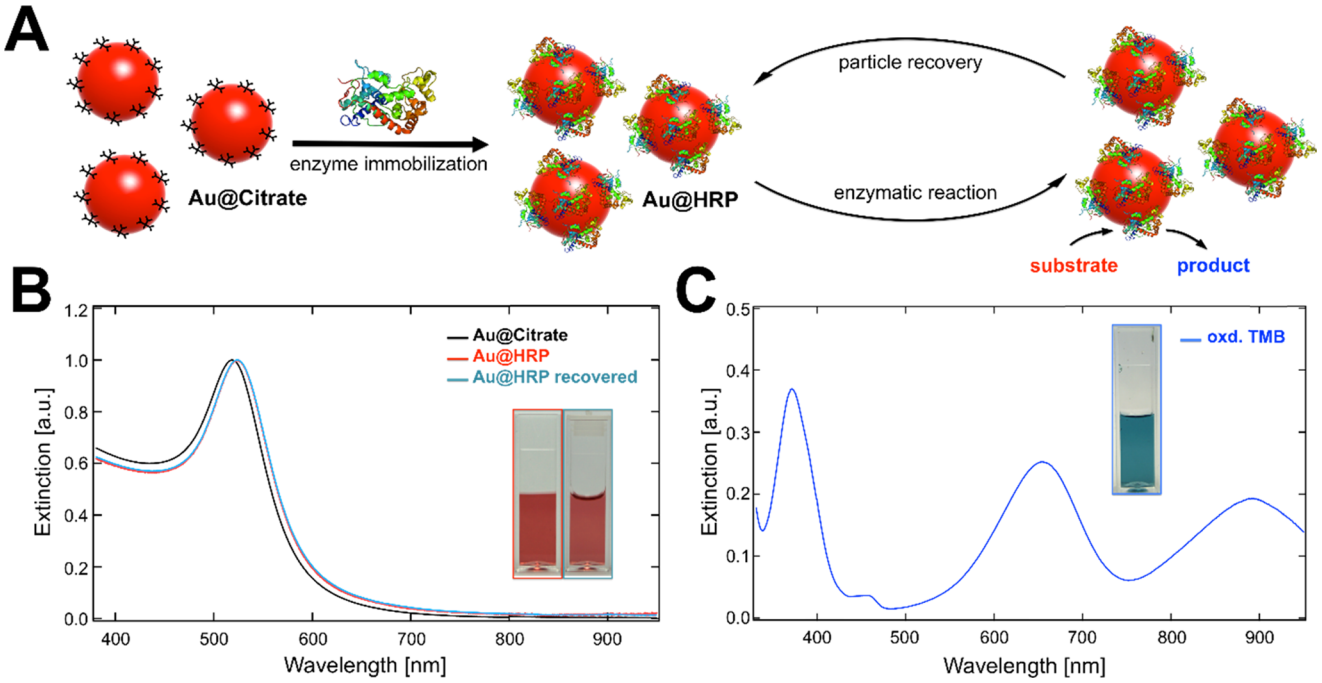

Figure 1. Preparation of catalytically (re-)active HRP-coated gold nanoparticles via physisorption (ligand-exchange reaction). (A) Schematic illustration of coating citrate-stabilized gold nanoparticles with HRP (Au@HRP) and the following enzymatic reaction. The Au@HRP can be recovered multiple times. (B) UV−vis spectra of Au@citrate (black), Au@HRP (red), and Au@HRP recovered after enzymatic reaction (light blue). The inset displays the Au@HRP particle dispersion as prepared (red box) and recovered Au@HRP particle dispersion after an enzymatic reaction (light blue box). (C) UV−vis spectrum of oxidized 3,3′,5,5′-tetramethylbenzidine (TMB) with the characteristic adsorption peaks of the blue one-electron oxidation product $TMB^{\bullet+}$ at 370 and 652 nm.

colloidal support.[9,34] The catalytic performance of the enzymes immobilized onto NPs can decrease drastically, due to hindered accessibility of the substrates to their active sites,[9] when the NPs are not stable and aggregate or sediment in the reaction media. Hence, to create a functional enzymatically active colloidal system, a robust enzyme immobilization on the NPs as well as a colloidally stable system is required.

Recently, we have reported a quite simple approach for a highly robust immobilization of proteins and enzymes onto metal and metal oxide NPs, simply via physisorption in a ligand-exchange process.[15,16,34,35,47−52] Different enzymes, such as horseradish peroxidase, glucose oxidase, laccase, and catalase, were directly immobilized onto plasmonic gold NPs and superparamagnetic iron oxide (Fe_3O_4) NPs, yielding colloidally stable enzyme-coated NP systems. The enzyme coating on the NP surface is highly robust and enzymatically active. The colloidal stability and enzymatic performance (V_{max}, K_m) of the enzyme-coated NPs (Au@enzyme) are strongly dependent on the pH of the dispersion and the physicochemical properties of the respective enzyme. Hence, gold NPs are particularly suitable for the immobilization of proteins and enzymes because of their plasmonic properties, allowing fast detection of NP aggregation upon color change of dispersions, owing to the plasmonic coupling.[15,16,35,47,49,51]

The present work represents a proof-of-principle study for an enzymatic colloidal system, based on HRP-coated gold NPs (Figure 1), being capable of catalyzing polymerization of different monomers, such as *N*-isopropylacrylamide (NIPAAM) and di(ethylene glycol)methyl ether methacrylate (DEGMA), yielding thermosensitive polymers (Figure 2). Furthermore, we show that the Au@HRP NPs can be recovered almost completely after each polymerization reaction simply via centrifugation or via sedimentation in case of larger particles (100 nm Au@HRP NPs) and then be reused in two further (or even more) successful polymerization cycles. To the best of our knowledge, a highly stable enzymatic colloidal system, which is capable of multiple use and facile recovery, based on immobilized enzymes on metal NPs as a complete new and sustainable approach in the field of polymer synthesis and colloidal enzymatic catalysis, has not been reported so far.

RESULTS AND DISCUSSION

Enzymatically (re-)active HRP-coated gold NPs (Au@HRP) of different sizes as reusable nanobiocatalysts were synthesized by coating the enzyme directly onto ∼15 and ∼100 nm citrate-stabilized gold NPs[34] (Figures 1 and S1−S5 in the Supporting Information (SI)). Upon enzyme immobilization, the localized surface plasmon resonance (LSPR) of the 15 nm NP (Au15@HRP) dispersions red shifts from 519 to 523.5 nm (Figure 1B) and from 554 to 557.5 nm for the larger NP (Au100@HRP), owing to refractive index changes in the vicinity of the NP surface. The occurring redshift of 4.5 nm (3.5 nm for larger Au100@HRP NPs) and no significant change in color or LSPR band broadening indicate a successful enzyme coating without any particle aggregation during the entire coating process. In contrast to the systems reported in the literature,[45,53] the HRP-coated gold NPs (Au@HRP) were purified from the free enzyme via several purification steps (i.e., five centrifugation/redispersion cycles).

In accordance with our previous work on protein and enzyme-coated NPs,[15,16,34,35] the final purified Au@HRP NPs exhibited high colloidal stability at pH 7.4 (Figure 1B), and the enzyme coating on the gold NPs was very robust and did not detach from the NP surface during the five purification cycles

DOI: 10.1021/acsomega.7b00700
ACS Omega 2017, 2, 7305−7312

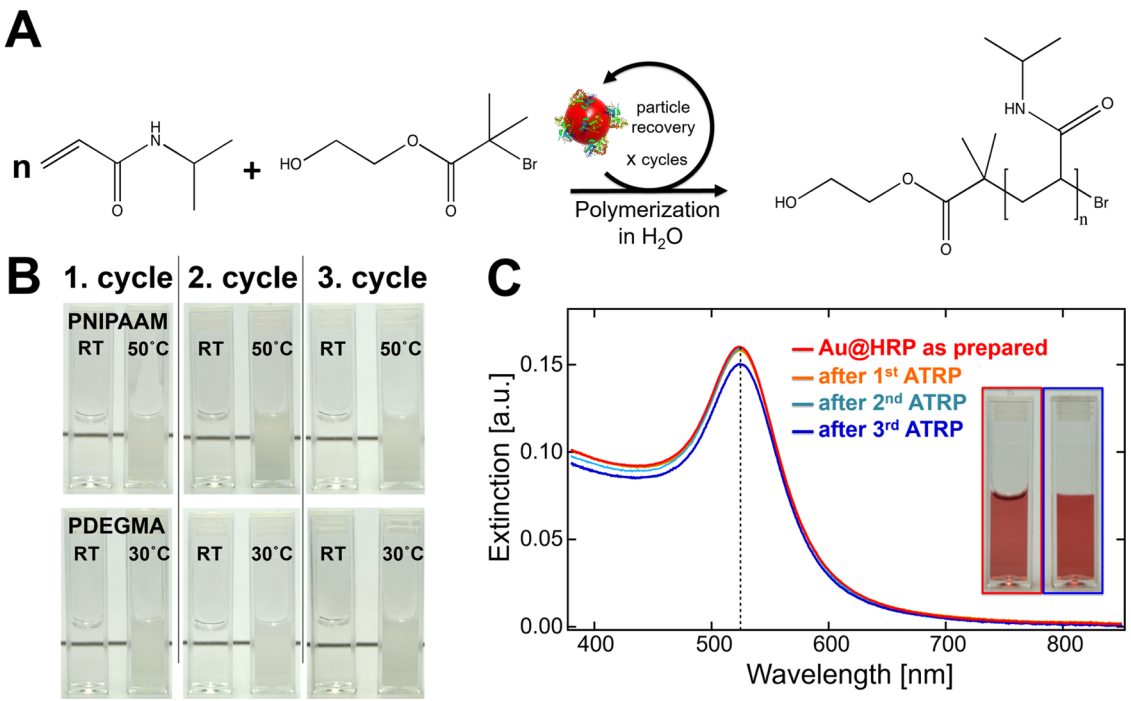

Figure 2. Au@HRP as recyclable nanobiocatalyst for polymerization reaction. (A) Examplified multicycle atom transfer radical polymerization (ATRP) process of NIPAAM using HRP-coated gold NPs as nanobiocatalyst with 2-hydroxyethyl 2-bromoisobutyrate (HEBIB) as ATRP initiator. Because the gold NPs can be recovered via centrifugation, they can be reused multiple times. (B) Visible evidence of polymer formation over all three polymerization cycles. Representative photographs of poly(*N*-isopropylacrylamide) (PNIPAAM) (upper row) and poly(di(ethylene glycol)methyl ether methacrylate) (PDEGMA) (lower row) in aqueous solution after removing the Au@HRP via centrifugation. The temperatures of the solutions are displayed on the vials (left: below lower critical solution temperature (LCST) = room temperature; right: above LCST = 50 °C for PNIPAAM and 30 °C for PDEGMA). (C) UV−vis spectra of the original Au@HRP (pH 7.4) and the recovered gold NPs during the individual three polymerization cycles of NIPAAM. The inset shows photographs of the original Au@HRP (red box, pH 7.4) and the recovered Au@HRP (blue box, pH 7.4) after the third polymerization of NIPAAM.

(the fifth supernatant shows no enzymatic activity). The HRP loading was experimentally determined, being ca. 21 HRP molecules per particle (for 15 nm NPs) and theoretically confirmed, as reported previously.[34] The catalytic activity of the Au@HRP NPs was checked by the oxidation of 3,3′,5,5′-tetramethylbenzidine (TMB) in the presence of H_2O_2 (Figure 1C). TMB is oxidized by the immobilized HRP in the presence of H_2O_2, yielding a blue-colored product ($TMB^{\bullet+}$) upon one-electron oxidation and/or a yellow-colored product (tetramethylbenzidine diimine) upon two-electron oxidation. An exemplary UV−vis spectrum of the oxidized TMB via Au@HRP NPs is shown in Figure 1C. A detailed and comparative study of the enzymatic activity parameters, that is, the Michaelis−Menten constants V_{max} and K_m, for the catalytic oxidation of TMB for both the immobilized enzyme (Au@HRP) and the native HRP can be found in our recent publication.[34]

The Au@HRP NPs were used as a reusable colloidal nanobiocatalyst in the polymerization of NIPAAM and DEGMA, yielding thermosensitive polymers with lower critical solution temperatures (LCST) of 32.5 °C[54,55] (PNIPAAM) and 28.0 °C[55] (PDEGMA). The successful formation of polymers can be easily identified at elevated temperatures due to precipitation of insoluble polymers above their LCST. The reaction conforms to the enzyme/ATRPase-catalyzed polymerization of such water-soluble monomers, as reported previously by Bruns et al.[6,7]

The catalytically (re-)active Au15@HRP NPs were used as nanobiocatalyst in the polymerization of NIPAAM and DEGMA under ATRP conditions, in the presence of sodium ascorbate as reducing agent and 2-hydroxyethyl 2-bromoisobutyrate (HEBIB) as typical ATRP initiator. After the reaction was quenched by exposing the solution to air, the Au15@HRP NPs were recovered by centrifugation (60 min, 8000 rcf) and reused in two further polymerization cycles under the same conditions, as illustrated in Figure 2A. Even after three polymerization cycles, the Au@HRP NPs remain catalytically active and retain their colloidal stability as proven by the color of the NP dispersion (Figure 2, blue-framed cuvette) and the LSPR band, which did not change in comparison to the as-prepared Au@HRP NPs (red-framed), before the polymerization reaction. Particle loss in the range of approximately 7−11% was recorded after three polymerization cycles (7.25% for NIPAAM, 10.75% for DEGMA), which is attributed to the various centrifugation steps for the recovery. Because both polymers exhibit an LCST, polymer formation was affirmed after each cycle by inducing polymer precipitation upon heating the final purified polymer solution above the respective LCST, which can be observed by the bare eye (Figure 2B).

To gain further insight into the performance of the Au@HRP NPs in the polymerization reaction over various cycles, the evolution of the molecular weight and molecular weight distribution was studied by gel permeation chromatography (GPC). The GPC measurements (Figure 3) revealed monomodal polymer weight distribution for both polymers PNIPAAM and PDEGMA. Furthermore, their molecular weights (M_n and M_w) and polydispersity indices (PDIs) are largely constant for the individual three polymerization cycles,

DOI: 10.1021/acsomega.7b00700
ACS Omega 2017, 2, 7305−7312

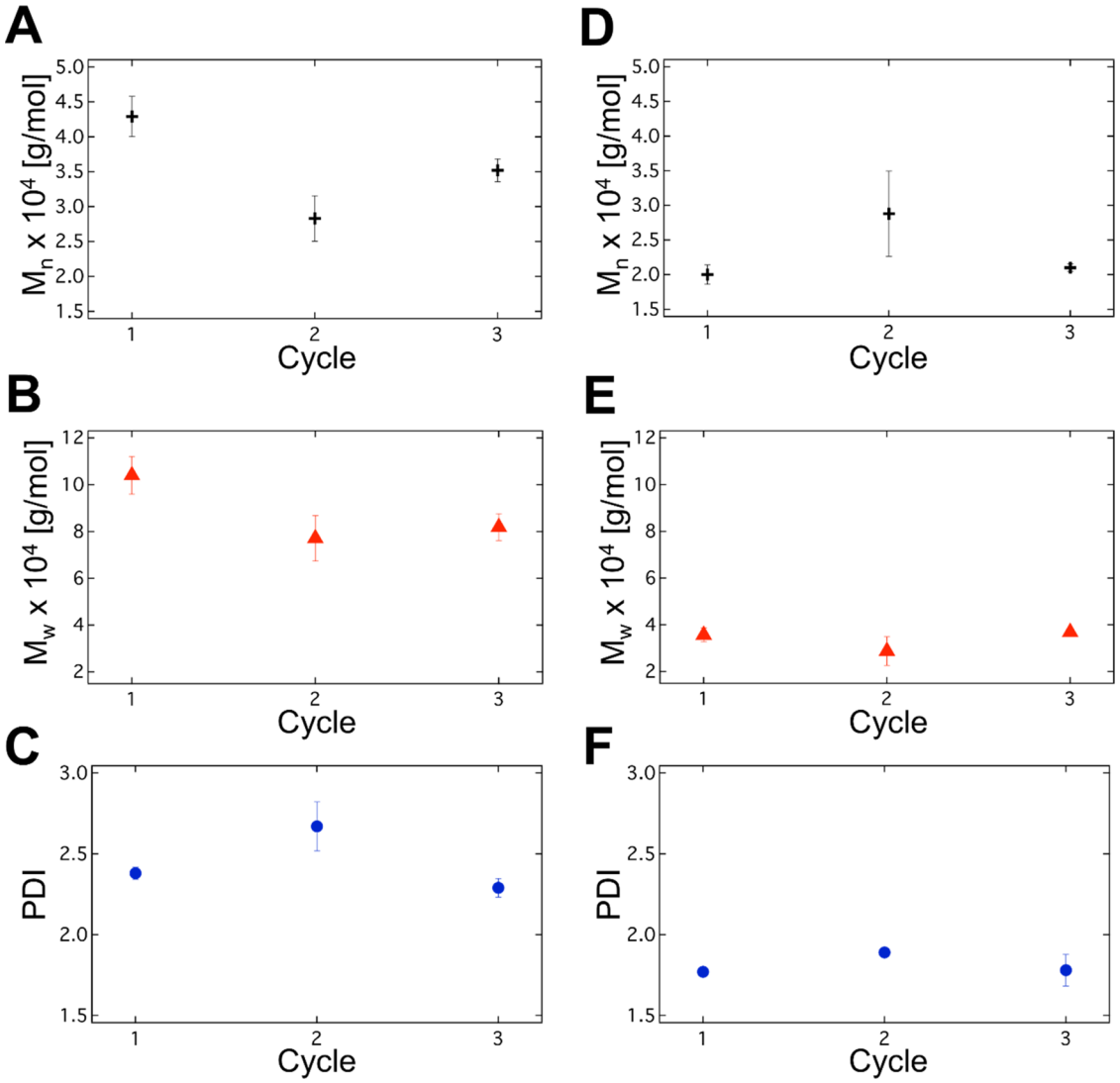

Figure 3. GPC results of polymerization of PNIPAAM and PDEGMA for three polymerization cycles using Au@HRP as nanobiocatalyst (error bars were determined via standard deviation of the three measurements). Left column shows the average values of M_n (A), M_w (B), and PDI (C) of PNIPAAM for all three polymerization cycles. Right column shows the average values of M_n (D), M_w (E), and PDI (F) of PDEGMA for all three polymerization cycles.

indicating that the catalytic performance of the immobilized HRP molecules could be maintained during the individual polymerization cycles. The exact values of M_n, M_w, and PDI are summarized in Table S1 in the Supporting Information. The results for molecular weight and PDI vary from the results reported in the literature.[6] One possible explanation could be the pH of 7.4 of the reaction medium, which is known to be not optimal for HRP-mediated reactions,[34] including (activators regenerated by electron transfer) ATRP.[6] Nevertheless, pH for the polymerization mixture was set to 7.4, to ensure colloidal stability (Figure 2C) of the nanobiocatalyst throughout the reaction.[34]

To gain a better insight into the polymerization reaction, reaction kinetics via ^{1}H NMR spectroscopy can be followed. However, for monitoring the kinetics via ^{1}H NMR spectroscopy, a total volume of 250 μL (which corresponds to 20 mg of specimen) per NMR sample is required. Because NIPAAM and DEGMA are rather small monomers (M_w = 113 g/mol for NIPAAM and M_w = 188 g/mol for DEGMA), high amount of monomers and catalyst (i.e., ca. 20-fold more) would be required to obtain enough polymer product for a systematic study. However, these upscaling challenges were avoided by using a macromonomer with a similar chemical structure, such as poly(ethylene glycol)methyl ether acrylate (PEGA, M_w: 480 g/mol). By using a high-molecular-weight monomer, the requirements of the ^{1}H NMR measurements could be somewhat fulfilled, without altering the monomer/catalyst ratio exorbitantly. Although, the Au@HRP NP-catalyzed polymerization of PEGA shows a linear correlation between reaction time and the negative natural logarithm of the conversion (for at least the first 5 h, Figure S6 in SI), suggesting that the polymerization follows a first-order kinetics. This indicates that the Au@HRP NP-catalyzed polymerization of PEGA follows somewhat the mechanism of a controlled radical polymerization, which is roughly in accordance with the results reported by Bruns et al. on pure HRP-mediated ATRP of NIPAAM.[6] Also the evolution of M_n and PDI follows roughly the trend in accordance with the pure HRP-mediated ATRP.[6] In view of these results and the complexity of the system, it becomes clear that reaction conditions for a

DOI: 10.1021/acsomega.7b00700
ACS Omega 2017, 2, 7305−7312

controlled polymerization reaction using Au@HRP NPs as colloidal catalysts have not been found yet. However, detailed studies with variation of various reaction parameters, such as the concentration of ingredients, type of ingredients, and environmental parameters (temperature, pH, buffer, salts), will be required to indentify the reaction mechanism and eventually achieve a well-controlled polymerization reaction. These studies are the subject of ongoing work.

CONCLUSIONS

We have demonstrated a simple and straightforward synthesis route of catalytically active HRP-coated gold nanoparticles that can be used as a reusable nanobiocatalyst in several polymerization cycles of vinyl monomers under reaction conditions that are typical for ATRP reactions. However, the M_w and PDI results indicate that the polymerization reactions do not follow a controlled polymerization pathway but rather a free-radical polymerization. Finding the right conditions for achieving a higher degree of control would be the focus of the upcoming reports. Nevertheless, the outstanding characteristic within this system is the simple recovery via centrifugation and reusability of the Au@HRP over multiple cycles. The colloidal stability of the enzyme-coated gold NPs was provided throughout the process, that is, during the enzyme-coating process and the three subsequent polymerization cycles. Furthermore, we were able to limit the particle loss down to 7.25% for the three polymerization cycles of NIPAAM (10.75% for the three polymerization cycles of DEGMA). The molecular weight and PDI, measured by GPC, of the obtained polymers show no significant changes within the individual cycles, indicating that the catalytic activity of the immobilized HRP molecules could be maintained during all polymerization cycles. In view of these results, the use of HRP-coated NPs as a reusable colloidal catalyst is highly feasible in more than just three polymerization cycles. Hence, the enzyme-coated NPs take the enzyme-catalyzed polymerization reactions from the regime of homogeneous catalysis to the regime of quasi-homogeneous catalysis, thus enabling facile separation of the macromolecular catalyst from the macromolecular product.

MATERIALS AND METHODS

Materials. Peroxidase from horseradish (HRP, lyophilized, powder; Sigma-Aldrich), bovine serum albumin (BSA, ≥98%), *N*-isopropylacrylamide (NIPAAM, 97%; Sigma-Aldrich), di(ethylene glycol)methyl ether methacrylate (DEGMA, 95%; Sigma-Aldrich), and poly(ethylene glycol)methyl ether acrylate (PEGA, average M_n = 480 g/mol; Sigma-Aldrich) were passed over aluminum oxide (neutral) prior to use to remove the inhibitor. 2-Hydroxyethyl 2-bromoisobutyrate (HEBIB, 95%; Sigma-Aldrich), (+)-sodium L-ascorbate (crystalline, ≥98%; Sigma-Aldrich), gold(III) chloride trihydrate (≥99.9% trace metal basis; Sigma-Aldrich), sodium citrate tribasic dihydrate (ACS reagent, ≥99.0%; Sigma-Aldrich), aluminum oxide (activated, neutral, Brockmann I; Sigma-Aldrich), phosphate-buffered saline (PBS, tablet; Sigma-Aldrich), sodium hydroxide (Grüssing GmbH), and 3,3′,5,5′-tetramethylbenzidine (Sigma-Aldrich) were used as received.

Methods. *Gel Permeation Chromatography (GPC).* The apparent number-average molecular weight (M_n) and weight-average molecular weight (M_w) based on polystyrene standards and the polydispersity index (PDI) of the yielded polymers were determined by GPC. Measurements of PNIPAAM, PDEGMA, and PEGA were performed on an Agilent 1260 Infinity series equipped with an autosampler, a diode array detector, and a refractive index detector. They were measured with a precolumn (GRAM 10 μm (8.0 × 50 mm^2)) and two main columns (GRAM 10 μm, 100 Å (8.0 × 300 mm^2) and GRAM 10 μm, 3000 Å (8.0 × 300 mm^2)) thermostatted to room temperature, using dimethylformamide (DMF, +5 g/L lithium bromide) as the mobile phase with a flow rate of 0.5 mL/min. The column setup was provided by Polymer Standards Service GmbH. GPC samples were prepared by dissolving the lyophilized polymer in DMF (polymer's concentration amounts to 2 mg/mL). After homogenization overnight, 20 μL of the samples was injected into the GPC device. The measurement time was 65 min.

^{1}H NMR. ^{1}H NMR spectroscopy was carried out with a Bruker Avance 300 (300 MHz) instrument. All measurements were performed at room temperature using deuterated dimethyl sulfoxide as solvent.

UV−Vis Spectroscopy. UV−vis spectra were acquired with a Specord Plus 250 (Analytik Jena) spectrophotometer. For measurements, 1.5 mL of the corresponding solution was placed in a cell and spectral analysis was performed in the 300−1100 nm range at room temperature.

Transmission Electron Microscopy (TEM). The average size, distribution, and morphology of citrate-stabilized AuNP and HRP-coated AuNP before and after every polymerization cycle were analyzed by TEM using a LEO 922 A EFTEM microscope (OMEGA). TEM samples were prepared by placing one drop of diluted aqueous dispersion of AuNP in a carbon-coated copper grid and allowing the solvent to evaporate at room temperature. The average particle diameter and distribution were determined by evaluating at least 300 individual particles using the software ImageJ.

Preparation of 15 nm Gold Nanoparticles (Au15@citrate). Gold NPs of about 15 nm in size were prepared by the citrate reduction method.[56] In a typical procedure, 750 mL of 0.25 mM $HAuCl_4$ solution was put in an Erlenmeyer flask and heated to boiling. Under vigorous stirring, 18 mL of a 1 wt % citrate solution was added, resulting in a color change of the solution from a grayish-blue to deep wine-red within 10 min. Now the heating is stopped and the solution cools down with stirring overnight. The resulting Au15@citrate was stored at 4 °C.

Preparation of 100 nm Gold Nanoparticles (Au100@Citrate). Quasi-spherical citrate-stabilized AuNPs with an average particle size of ∼100 nm were synthesized by the citrate reduction-based seeded growth method developed by Puntes et al.[57] In a 250 mL three-neck round-bottom flask, 150 mL of a 2.2 mM aqueous solution of sodium citrate was heated in an oil bath for 15 min under reflux and vigorous stirring at permanent control of the solution temperature. At 100 °C, 1 mL of a 25 mM $HAuCl_4$ solution was immediately injected, by which the color of the solution changed from yellow to bluish-gray and then to soft pink within 10 min. The resulting citrate-stabilized AuNPs were used as seeds for the next seeded growth steps by successive addition of Au precursor, citrate solution, Milli-Q water, and dilution steps as reported elsewhere.[57] After 11 consecutive growth steps, citrate-stabilized 100 nm AuNPs were obtained. The resulting NPs were stored at 4 °C.

Immobilization of HRP onto Gold Nanoparticles. For preparation of an HRP solution, 2 mg of HRP is dissolved in 10 mL of a 0.1 wt % citrate solution. Subsequently, 90 mL of a filtered (Nylon, 0.1 μm) particle solution (9.1 × 10^{-5} M, pH =

DOI: 10.1021/acsomega.7b00700
ACS Omega 2017, 2, 7305−7312

9) is added dropwise under stirring to the protein solution (final HRP concentration of 0.02 mg/mL). The protein/particle solution is stirred overnight and afterward purified by five centrifugation steps (60 min, 8000 rcf; 4 °C). After every centrifugation step, the gold NPs are redispersed in basic water (pH = 9). The supernatant of the fifth centrifugation cycle was checked on enzymatic activity and enzyme desorption from the NPs surface via TMB oxidation.

Activity Measurements of Au15@HRP. Activity measurements of Au@HRP NPs were performed following the procedures reported elsewhere.[34]

ATRP of NIPAAM and DEGMA Using Au15@HRP as Nanobiocatalyst. The polymerization was carried out in 100 mM PBS solution at pH 7.4. HEBIB (2.4 μL, 3.5 mg, 16.5 μmol) and monomer (NIPAAM: 127.5 mg, 1.127 mmol; DEGMA: 121.1 mg, 207.9 μL, 1.127 mmol; NIPAAM was used as received; DEGMA was passed over aluminum oxide (neutral) prior to use to remove the inhibitor) were weighed in a flask and dissolved in 3.75 mL of PBS buffer. In two separate flasks, sodium ascorbate (7.5 mg, 37.9 μmol) was dissolved in 2.5 mL of PBS buffer and 1 mL of an HRP-coated gold NP solution ([Au^0] = 4 mM) was weighed. Au15@HRP was obtained from a stock solution, and its concentration was measured via UV−vis spectroscopy. Oxygen was removed from all three flasks by purging the solutions with nitrogen for 20−30 min. The monomer/initiator mixture (750 μL) was syringed to the gold NP solution and then the polymerization was started by transferring 250 μL of the reducing agent solution into the Au15@HRP/NIPAAM/HEBIB solution in the vial by means of a syringe. The ratio of reactants in the reaction mixture was 1/68/1.1/1212 (HEBIB/monomer/sodium ascorbate/Au15@HRP (# NPs)). The reaction was stirred at room temperature under nitrogen atmosphere for 2.5 h. Subsequently, the polymerization was quenched by exposing the reaction to air, and the Au15@HRP NPs were removed from the solution by several centrifugation steps (60 min, 8000 rcf). After every centrifugation cycle, the Au15@HRP NPs were rinsed with PBS. The recovered gold NPs were used in two further polymerization cycles under the same conditions. The successful polymer formation can be easily confirmed due to precipitation of insoluble polymer above its LCST. Molecular weight and PDI of the polymer chains were investigated with GPC. Every data point was calculated out of three individual polymerizations. The uncertainty of the GPC device was in the range of 12−12.9%.

Polymerization of PEGA Using Au15@HRP as Nanobiocatalyst. The polymerization of PEGA using Au15@HRP as biocatalyst was carried out analogously to the polymerization of NIPAAM and DEGMA. HEBIB (4.19 μL, 6.1 mg, 28.89 μmol) and PEGA (1.08 g, 0.992 mL, 2.25 mmol, PEGA was passed over aluminum oxide (neutral) prior to use to remove the inhibitor) were weighed in a flask and dissolved in 3.0 mL of PBS buffer (pH = 7.4). In two separate flasks, sodium ascorbate (1.73 mg, 158.3 μmol) was dissolved in 2.5 mL of PBS buffer (pH = 7.4) and 2 mL of an Au15@HRP solution ([Au^0] = 4 mM) was weighed. Oxygen was removed from all three flasks by purging the solutions with nitrogen for 30 min. The monomer/initiator mixture (2.5 mL) was syringed to the AuNP solution. Subsequently, polymerization was started by transferring 1 mL of the reducing agent solution into the Au15@HRP/PEGA/HEBIB solution by means of a syringe. The ratio of the reactants was 1/79/1.4/332 (HEBIB/PEGA/sodium ascorbate/Au15@HRP). Samples (250 μL) were taken in periodical time intervals to track the conversion rate via ^{1}H NMR spectroscopy.

■ ASSOCIATED CONTENT

Supporting Information

The Supporting Information is available free of charge on the ACS Publications website at DOI: 10.1021/acsomega.7b00700.

Sedimentation (recovery) behavior and colloidal stability (redispersion) of larger HRP-coated gold NPs with an average size of 100 nm (Au100@HRP NPs); TEM images of citrate-stabilized and HRP-coated gold nanoparticles ($d \sim 15$ nm) before and after three polymerization cycles; TEM images of larger HRP-coated gold NPs (Au100@HRP NPs); kinetic measurement of polymerization of PEGA with Au15@HRP NPs; table summarizing M_w and PDI results of the polymerization of NIPAM and DEGMA with Au15@HRP NPs (PDF)

■ AUTHOR INFORMATION

Corresponding Author

*E-mail: chananam@ethz.ch.

ORCID

Munish Chanana: 0000-0002-0736-0119

Notes

The authors declare no competing financial interest.

■ ACKNOWLEDGMENTS

J.S. was supported and funded by a grant for Ph.D. candidates of the German Federal Environmental Foundation (DBU). The authors thank Bianca Uch for the GPC measurements, Kerstin Hannemann for NMR measurements, and Prof. Dr. Andreas Fery for fruitful discussions and his support.

■ REFERENCES

(1) Kalra, B.; Gross, R. A. Horseradish Peroxidase Mediated Free Radical Polymerization of Methyl Methacrylate. *Biomacromolecules* **2000**, *1*, 501−505.

(2) Gross, R. A.; Kumar, A.; Kalra, B. Polymer Synthesis by In Vitro Enzyme Catalysis. *Chem. Rev.* **2001**, *101*, 2097−2124.

(3) Bornscheuer, U. T.; Huisman, G. W.; Kazlauskas, R. J.; Lutz, S.; Moore, J. C.; Robins, K. Engineering the third wave of biocatalysis. *Nature* **2012**, *485*, 185−194.

(4) Ng, Y.-H.; di Lena, F.; Chai, C. L. L. Metalloenzymatic radical polymerization using alkyl halides as initiators. *Polym. Chem.* **2011**, *2*, 589−594.

(5) Ng, Y.-H.; di Lena, F.; Chai, C. L. L. PolyPEGA with predetermined molecular weights from enzyme-mediated radical polymerization in water. *Chem. Commun.* **2011**, *47*, 6464−6466.

(6) Sigg, S. J.; Seidi, F.; Renggli, K.; Silva, T. B.; Kali, G.; Bruns, N. Horseradish Peroxidase as a Catalyst for Atom Transfer Radical Polymerization. *Macromol. Rapid Commun.* **2011**, *32*, 1710−1715.

(7) Silva, T. B.; Spulber, M.; Kocik, M. K.; Seidi, F.; Charan, H.; Rother, M.; Sigg, S. J.; Renggli, K.; Kali, G.; Bruns, N. Hemoglobin and Red Blood Cells Catalyze Atom Transfer Radical Polymerization. *Biomacromolecules* **2013**, *14*, 2703−2712.

(8) Dinu, M. V.; Spulber, M.; Renggli, K.; Wu, D.; Monnier, C. A.; Petri-Fink, A.; Bruns, N. Filling Polymersomes with Polymers by Peroxidase-Catalyzed Atom Transfer Radical Polymerization. *Macromol. Rapid Commun.* **2015**, *36*, 507−514.

(9) Abu-Reziq, R.; Alper, H. Magnetically Separable Base Catalysts: Heterogeneous Catalysis vs. Quasi-Homogeneous Catalysis. *Appl. Sci.* **2012**, *2*, 260.

DOI: 10.1021/acsomega.7b00700
ACS Omega 2017, 2, 7305−7312

(10) Astruc, D.; Lu, F.; Aranzaes, J. R. Nanoparticles as Recyclable Catalysts: The Frontier between Homogeneous and Heterogeneous Catalysis. *Angew. Chem., Int. Ed.* **2005**, *44*, 7852−7872.
(11) Jia, C.-J.; Schuth, F. Colloidal metal nanoparticles as a component of designed catalyst. *Phys. Chem. Chem. Phys.* **2011**, *13*, 2457−2487.
(12) Prati, L.; Villa, A. Gold Colloids: From Quasi-Homogeneous to Heterogeneous Catalytic Systems. *Acc. Chem. Res.* **2014**, *47*, 855−863.
(13) Ahmad, A.; Sardar, M. Enzyme Immobilization: An Overview on Nanoparticles as Immobilization. *Biochem. Anal. Biochem.* **2015**, *4*, 178.
(14) Mohamad, N. R.; Marzuki, N. H. C.; Buang, N. A.; Huyop, F.; Wahab, R. A. An overview of technologies for immobilization of enzymes and surface analysis techniques for immobilized enzymes. *Biotechnol. Biotechnol. Equip.* **2015**, *29*, 205−220.
(15) Chanana, M.; RiveraGil, P.; Correa-Duarte, M. A.; Liz-Marzán, L. M.; Parak, W. J. Physicochemical Properties of Protein-Coated Gold Nanoparticles in Biological Fluids and Cells before and after Proteolytic Digestion. *Angew. Chem., Int. Ed.* **2013**, *52*, 4179−4183.
(16) Dewald, I.; Isakin, O.; Schubert, J.; Kraus, T.; Chanana, M. Protein Identity and Environmental Parameters Determine the Final Physicochemical Properties of Protein-Coated Metal Nanoparticles. *J. Phys. Chem. C* **2015**, *119*, 25482−25492.
(17) Akbulut, O.; Mace, C. R.; Martinez, R. V.; Kumar, A. A.; Nie, Z.; Patton, M. R.; Whitesides, G. M. Separation of Nanoparticles in Aqueous Multiphase Systems through Centrifugation. *Nano Lett.* **2012**, *12*, 4060−4064.
(18) Kim, Y. C.; Han, S.; Hong, S. A feasibility study of magnetic separation of magnetic nanoparticle for forward osmosis. *Water Sci. Technol.* **2011**, *64*, 469−476.
(19) Garcia-Galan, C.; Berenguer-Murcia, Á; Fernandez-Lafuente, R.; Rodrigues, R. C. Potential of Different Enzyme Immobilization Strategies to Improve Enzyme Performance. *Adv. Synth. Catal.* **2011**, *353*, 2885−2904.
(20) Liu, W.; Wang, L.; Jiang, R. Specific Enzyme Immobilization Approaches and Their Application with Nanomaterials. *Top. Catal.* **2012**, *55*, 1146−1156.
(21) Brennan, J. L.; Hatzakis, N. S.; Tshikhudo, T. R.; Razumas, V.; Patkar, S.; Vind, J.; Svendsen, A.; Nolte, R. J. M.; Rowan, A. E.; Brust, M.; Dirvianskyte, N. Bionanoconjugation via Click Chemistry: The Creation of Functional Hybrids of Lipases and Gold Nanoparticles. *Bioconjugate Chem.* **2006**, *17*, 1373−1375.
(22) Karaaslan, M. A.; Gao, G.; Kadla, J. F. Nanocrystalline cellulose/β-casein conjugated nanoparticles prepared by click chemistry. *Cellulose* **2013**, *20*, 2655−2665.
(23) Montalbetti, C. A. G. N.; Falque, V. Amide bond formation and peptide coupling. *Tetrahedron* **2005**, *61*, 10827−10852.
(24) Joullie, M. M.; Lasse, K. M. Evolution of amide bond formation. Commemorative Issue in Honor of Dr. Bruce E. Maryanoff on the occasion of his outstanding contributions to organic chemistry as an industrial chemist. *Arch. Org. Chem.* **2010**, *2010*, 189−250.
(25) Pattabiraman, V. R.; Bode, J. W. Rethinking amide bond synthesis. *Nature* **2011**, *480*, 471−479.
(26) Li, F.; Li, J.; Zhang, S. Molecularly imprinted polymer grafted on polysaccharide microsphere surface by the sol−gel process for protein recognition. *Talanta* **2008**, *74*, 1247−1255.
(27) Coad, B. R.; Vasilev, K.; Diener, K. R.; Hayball, J. D.; Short, R. D.; Griesser, H. J. Immobilized Streptavidin Gradients as Bioconjugation Platforms. *Langmuir* **2012**, *28*, 2710−2717.
(28) Hanefeld, U.; Gardossi, L.; Magner, E. Understanding enzyme immobilisation. *Chem. Soc. Rev.* **2009**, *38*, 453−468.
(29) Sheldon, R. A. Cross-linked enzyme aggregates (CLEAs): stable and recyclable biocatalysts. *Biochem. Soc. Trans.* **2007**, *35*, 1583−1587.
(30) Sardar, M.; Gupta, M. N. Immobilization of tomato pectinase on Con A−Seralose 4B by bioaffinity layering. *Enzyme Microb. Technol.* **2005**, *37*, 355−359.
(31) Shi, Q.-H.; Tian, Y.; Dong, X.-Y.; Bai, S.; Sun, Y. Chitosan-coated silica beads as immobilized metal affinity support for protein adsorption. *Biochem. Eng. J.* **2003**, *16*, 317−322.
(32) Lei, C.; Shin, Y.; Liu, J.; Ackerman, E. J. Entrapping Enzyme in a Functionalized Nanoporous Support. *J. Am. Chem. Soc.* **2002**, *124*, 11242−11243.
(33) Wen, H.; Nallathambi, V.; Chakraborty, D.; Barton, S. C. Carbon fiber microelectrodes modified with carbon nanotubes as a new support for immobilization of glucose oxidase. *Microchim. Acta* **2011**, *175*, 283−289.
(34) Männel, M. J.; Kreuzer, L. P.; Goldhahn, C.; Schubert, J.; Hartl, M. J.; Chanana, M. Catalytically Active Protein Coatings: Towards Enzymatic Cascade Reactions at Inter-Colloidal Level. *ACS Catal.* **2017**, *7*, 1664−1672.
(35) Strozyk, M. S.; Chanana, M.; Pastoriza-Santos, I.; Pérez-Juste, J.; Liz-Marzán, L. M. Stimuli-Responsive Materials: Protein/Polymer-Based Dual-Responsive Gold Nanoparticles with pH-Dependent Thermal Sensitivity (Adv. Funct. Mater. 7/2012). *Adv. Funct. Mater.* **2012**, *22*, 1322.
(36) Ward, K.; Xi, J.; Stuckey, D. C. Immobilization of enzymes using non-ionic colloidal liquid aphrons (CLAs): Activity kinetics, conformation, and energetics. *Biotechnol. Bioeng.* **2016**, *113*, 970−978.
(37) Lei, C.; Soares, T. A.; Shin, Y.; Liu, J.; Ackerman, E. J. Enzyme specific activity in functionalized nanoporous supports. *Nanotechnology* **2008**, *19*, No. 125102.
(38) Guzik, U.; Hupert-Kocurek, K.; Wojcieszyńska, D. Immobilization as a Strategy for Improving Enzyme Properties-Application to Oxidoreductases. *Molecules* **2014**, *19*, 8995.
(39) Katchalski, E.; Silman, I.; Goldman, R. Effect of the Microenvironment on the Mode of Action of Immobilized Enzymes. In *Advances in Enzymology and Related Areas of Molecular Biology*; John Wiley & Sons, Inc., 2006; pp 445−536.
(40) López-Serrano, P.; Cao, L.; van Rantwijk, F.; Sheldon, R. A. Cross-linked enzyme aggregates with enhanced activity: application to lipases. *Biotechnol. Lett.* **2002**, *24*, 1379−1383.
(41) Rodrigues, R. C.; Ortiz, C.; Berenguer-Murcia, Á.; Torres, R.; Fernández-Lafuente, R. Modifying enzyme activity and selectivity by immobilization. *Chem. Soc. Rev.* **2013**, *42*, 6290−6307.
(42) Subrizi, F.; Crucianelli, M.; Grossi, V.; Passacantando, M.; Pesci, L.; Saladino, R. Carbon Nanotubes as Activating Tyrosinase Supports for the Selective Synthesis of Catechols. *ACS Catal.* **2014**, *4*, 810−822.
(43) Zhang, Y.; Ge, J.; Liu, Z. Enhanced Activity of Immobilized or Chemically Modified Enzymes. *ACS Catal.* **2015**, *5*, 4503−4513.
(44) Kress, J.; Zanaletti, R.; Amour, A.; Ladlow, M.; Frey, J. G.; Bradley, M. Enzyme Accessibility and Solid Supports: Which Molecular Weight Enzymes Can Be Used on Solid Supports? An Investigation Using Confocal Raman Microscopy. *Chem. − Eur. J.* **2002**, *8*, 3769−3772.
(45) Wu, H.; Liu, Y.; Li, M.; Chong, Y.; Zeng, M.; Lo, Y. M.; Yin, J.-J. Size-dependent tuning of horseradish peroxidase bioreactivity by gold nanoparticles. *Nanoscale* **2015**, *7*, 4505−4513.
(46) Lundqvist, M.; Sethson, I.; Jonsson, B.-H. Protein Adsorption onto Silica Nanoparticles: Conformational Changes Depend on the Particles' Curvature and the Protein Stability. *Langmuir* **2004**, *20*, 10639−10647.
(47) Chanana, M.; Correa-Duarte, M. A.; Liz-Marzán, L. M. Insulin-Coated Gold Nanoparticles: A Plasmonic Device for Studying Metal−Protein Interactions. *Small* **2011**, *7*, 2650−2660.
(48) Hanske, C.; Tebbe, M.; Kuttner, C.; Bieber, V.; Tsukruk, V. V.; Chanana, M.; König, T. A. F.; Fery, A. Strongly Coupled Plasmonic Modes on Macroscopic Areas via Template-Assisted Colloidal Self-Assembly. *Nano Lett.* **2014**, *14*, 6863−6871.
(49) Höller, R. P. M.; Dulle, M.; Thomä, S.; Mayer, M.; Steiner, A. M.; Förster, S.; Fery, A.; Kuttner, C.; Chanana, M. Protein-Assisted Assembly of Modular 3D Plasmonic Raspberry-like Core/Satellite Nanoclusters: Correlation of Structure and Optical Properties. *ACS Nano* **2016**, *10*, 5740−5750.
(50) Moerz, S. T.; Kraegeloh, A.; Chanana, M.; Kraus, T. Formation Mechanism for Stable Hybrid Clusters of Proteins and Nanoparticles. *ACS Nano* **2015**, *9*, 6696−6705.

DOI: 10.1021/acsomega.7b00700
ACS Omega 2017, 2, 7305−7312

(51) Tebbe, M.; Kuttner, C.; Männel, M.; Fery, A.; Chanana, M. Colloidally Stable and Surfactant-Free Protein-Coated Gold Nanorods in Biological Media. *ACS Appl. Mater. Interfaces* **2015**, *7*, 5984−5991.
(52) Tebbe, M.; Mayer, M.; Glatz, B. A.; Hanske, C.; Probst, P. T.; Müller, M. B.; Karg, M.; Chanana, M.; König, T. A. F.; Kuttner, C.; Fery, A. Optically anisotropic substrates via wrinkle-assisted convective assembly of gold nanorods on macroscopic areas. *Faraday Discuss.* **2015**, *181*, 243−260.
(53) Ni, Y.; Li, J.; Huang, Z.; He, K.; Zhuang, J.; Yang, W. Improved activity of immobilized horseradish peroxidase on gold nanoparticles in the presence of bovine serum albumin. *J. Nanopart. Res.* **2013**, *15*, No. 2038.
(54) Heskins, M.; Guillet, J. E. Solution Properties of Poly(*N*-isopropylacrylamide). *J. Macromol. Sci., Chem.* **1968**, *2*, 1441−1455.
(55) Teixeira, F.; Popa, A. M.; Guimond, S.; Hegemann, D.; Rossi, R. M. Synthesis of poly(oligo(ethylene glycol)methacrylate)-functionalized membranes for thermally controlled drug delivery. *J. Appl. Polym. Sci.* **2013**, *129*, 636−643.
(56) Turkevich, J.; Stevenson, P. C.; Hillier, J. A study of the nucleation and growth processes in the synthesis of colloidal gold. *Discuss. Faraday Soc.* **1951**, *11*, 55−75.
(57) Bastús, N. G.; Comenge, J.; Puntes, V. Kinetically Controlled Seeded Growth Synthesis of Citrate-Stabilized Gold Nanoparticles of up to 200 nm: Size Focusing versus Ostwald Ripening. *Langmuir* **2011**, *27*, 11098−11105.

DOI: 10.1021/acsomega.7b00700
ACS Omega 2017, 2, 7305−7312